Article

Fault Detection and Isolation for Nonlinear Process Systems Using Asynchronous Measurements

Charles W. McFall, David Mun#oz de la Pen#a, Ben Ohran, Panagiotis D. Christofides, and James F. Davis

Ind. Eng. Chem. Res., **2008**, 47 (24), 10009-10019 • Publication Date (Web): 19 November 2008

Fault Detection and Isolation for Nonlinear Process Systems Using Asynchronous Measurements

Charles W. McFall, David Muñoz de la Peña, Ben Ohran, Panagiotis D. Christofides,* and James F. Davis

Department of Chemical and Biomolecular Engineering, University of California, Los Angeles, California 90095

This work addresses the problem of fault detection and isolation for nonlinear processes when some process variable measurements are available at regular sampling intervals and the remaining process variables are measured at an asynchronous rate. First, a fault detection and isolation (FDI) scheme that employs model-based techniques is proposed that allows for the isolation of faults. The proposed FDI scheme provides detection and isolation of any fault that enters into the differential equation of only synchronously measured states and grouping of faults that enter into the differential equation of any asynchronously measured state. For a fully coupled process system, fault detection occurs shortly after a fault takes place, and fault isolation, limited by the arrival of asynchronous measurements, occurs when asynchronous measurements become available. Fault-tolerant control methods with a supervisory control component are then employed to achieve stability in the presence of actuator failures using control system reconfiguration. Numerical simulations of a polyethylene reactor are performed to demonstrate the applicability and performance of the proposed fault detection and isolation and fault-tolerant control method in the presence of asynchronous measurements.

1. Introduction

Automation is a key component to the operation of any modern chemical process because it helps deal with environmental, safety, and economic concerns in real time. Increased levels of automation, however, may leave a chemical process vulnerable to failures such as actuator faults, sensor errors, or controller faults that may lead to waste of energy or feedstock and in some cases environmental and/or safety problems. At least 10 billion USD are lost annually in the US due to abnormal situations in chemical and process industries;[1] thus, timely detection and isolation and efficient handling of these situations are of critical importance. This work addresses the issue of handling abnormal situations considering that process measurements used for feedback control and process monitoring are typically asynchronous. This can be due to the nature of the measurement itself (i.e., concentration measurements may be difficult to obtain while temperature measurements are usually readily available) or due to the use of sensor networks (wired or wireless) that may introduce complex dynamics into the monitoring system due to field interference.

The first component required to develop a control scheme that is robust to failures is automatic fault detection and isolation (FDI) that will find the source of failures in a timely manner. Data-based methods for FDI utilize statistical and pattern recognition techniques for data analysis and interpretation.[2−13] Historical plant data are used to construct data-based indicators that identify deviations from normal operation to detect faults. There are also extensive model-based FDI results for linear systems,[14−18] and more recently, results have become available on nonlinear model-based FDI for broad classes of nonlinear systems.[19−23] Additionally, recent work has been done to improve fault threshold selection[24] in order to reduce FDI system response time. These works, in general, rely on measurements that are continuously or synchronously sampled, and they do not account for measurements that arrive asynchronously. Recently, research has been done on the topic of feedback control with asynchronous measurements.[25−28] These efforts provide a starting framework for control subject to asynchronous measurements, but they do not include FDI. The goal of this work is to develop an FDI scheme given asynchronous measurements that will allow fault-tolerant control (FTC) to take place.

One method to achieve fault-tolerant control is to implement more than the minimum number of feedback loops required to stabilize a given process. In the event of a failure in one or several of these feedback loops the remaining well-functioning feedback loops can maintain the desired closed-loop system stability and performance properties.[29−31] However, it is more economical, in terms of actuator energy, to operate the minimum number of feedback loops required to achieve the desired level of process control. Such a control system is, however, more vulnerable in the event of a failure because there are no active redundant feedback loops. This motivates the implementation of an FTC scheme that will automatically reconfigure the system to a dormant fall-back control configuration that guarantees process stability in the event of a failure.[21,22,26,32]

This work addresses the problem of fault detection and isolation and fault-tolerant control when process measurements are available at asynchronous time instants. First, a fault detection and isolation (FDI) scheme that employs model-based techniques is proposed that allows for the isolation of faults. This scheme employs model-based FDI filters similar to those found in ref 21 in addition to observers that estimate the fault-free evolution of asynchronously measured states during time intervals in which their measurements are not available. Specifically, the proposed FDI scheme provides detection and isolation of any fault that enters into the differential equation of only synchronously measured states and grouping of faults that enter into the differential equation of any asynchronously measured state. For a fully coupled process system, fault detection occurs shortly after a fault takes place, and fault isolation, limited by the arrival of asynchronous measurements, occurs when asynchronous measurements become available. Once the FDI methodology has provided the system supervisor with a fault diagnosis, the supervisor takes appropriate action to seamlessly

* Corresponding author. E-mail: pdc@seas.ucla.edu.

10.1021/ie801056y CCC: $40.75
Published on Web 11/19/2008

reconfigure the system to an alternative control configuration that will enforce the desired operation. We present applications of the proposed asynchronous FDI and FTC framework to a polyethylene reactor simulation.[33] Specifically, the polyethylene reactor includes seven state variables such as temperatures, species concentrations, and catalyst activity. This polyethylene plant naturally gives rise to measurements that can be sampled synchronously (such as temperature) and those that are sampled asynchronously (such as reactant and catalyst concentrations). Previous work of our group[34] considered fault-tolerant control of the polyethylene reactor assuming that all process variables are continuously measured. In the present work, it is shown through a detailed simulation study that the proposed model-based asynchronous FDI technique can lead to reliable actuator fault detection and isolation and fault-tolerant control in a timely manner.

2. FDI Using Asynchronous Measurements: Problem Formulation and Solution

2.1. Class of Nonlinear Systems. In this work, we consider nonlinear process systems described by the following state-space model

$$\begin{aligned}
\dot{x}_1 &= f_1(x_1, ..., x_{n_s}, x_{n_s+1}, ..., x_{n_s+n_a}, u, d_1, ..., d_p)\\
&\vdots\\
\dot{x}_{n_s} &= f_{n_s}(x_1, ..., x_{n_s}, x_{n_s+1}, ..., x_{n_s+n_a}, u, d_1, ..., d_p)\\
\dot{x}_{n_s+1} &= f_{n_s+1}(x_1, ..., x_{n_s}, x_{n_s+1}, ..., x_{n_s+n_a}, u, d_1, ..., d_p)\\
&\vdots\\
\dot{x}_{n_s+n_a} &= f_{n_s+n_a}(x_1, ..., x_{n_s}, x_{n_s+1}, ..., x_{n_s+n_a}, u, d_1, ..., d_p)
\end{aligned} \tag{1}$$

where $x_i \in R$ with $i = 1, ..., n_s$ denotes the set of state variables that are sampled synchronously, $x_i \in R$ with $i = n_s + 1, ..., n_s + n_a$ denotes the set of state variables that are sampled asynchronously, $u \in R^{n_u}$ denotes the input, and $d_i \in R$ with $i = 1, ..., p$ is a model of the set of p possible faults. The faults in d_i include actuator faults and disturbances and can take any value. For the purposes of the present work, it is necessary to know and include beforehand all of the potential faults in d. However, it should be noted that d is not limited and can include any number of faults. The consideration of adaptive learning methods to isolate unknown faults is outside of the scope of this work. The state of the system is given by the vector

$$x = \begin{bmatrix} x_1 \\ \vdots \\ x_{n_s} \\ x_{n_s+1} \\ \vdots \\ x_{n_s+n_a} \end{bmatrix} \in R^{n_s+n_a}$$

Using this definition for x, (1) can be written in the following equivalent compact form

$$\dot{x} = f(x, u, d_1, ..., d_p) \tag{2}$$

We assume that f is a locally Lipschitz vector function and that $f(0, 0, 0, ..., 0) = 0$. This means that the origin is an equilibrium point for the fault-free system with $u(t) \equiv 0$. Moreover, we assume that the fault-free system (system (1) with $d_i(t) \equiv 0$ for all t) has an asymptotically stable equilibrium at the origin $x = 0$ for a given feedback control h: $R^{n_s+n_a} \rightarrow R^{n_u}$ which satisfies $h(0) = 0$.

Remark 1. The assumption of existence of a stabilizing feedback law $h(x)$ is equivalent to the existence of a control Lyapunov function (CLF) for the system $\dot{x} = f(x, u, 0, ..., 0)$. Explicit stabilizing control laws that provide explicitly defined regions of attraction for the closed-loop system have been developed using Lyapunov techniques for specific classes of nonlinear systems, particularly input−affine nonlinear systems; the reader may refer to refs 35 and 36 for results in this area. In section 3, a method such as the one presented in ref 37 is used for the design of $h(x)$.

2.2. Modeling of Asynchronous Measurements. System (1) is controlled using both sampled synchronous and asynchronous measurements. We assume that $x_i(t) \in R$ with $i = 1, ..., n_s$ are sampled continuously (i.e., at intervals of fixed size $\Delta > 0$ where Δ is a sufficiently small positive number). Each state $x_i \in R$ with $i = n_s + 1, ..., n_s + n_a$ is sampled asynchronously and is only available at time instants $t_{k,i}$ where $t_{k\geq 0,i}$ is a random increasing sequence of times. A controller design that takes advantage of the asynchronous measurements must take into account that it will have to operate without complete state information between asynchronous samples. This class of systems arises naturally in process control, where process variables such as temperature, flow, or concentration have to be measured. In such a case, temperature and flow measurements can be assumed to be available continuously. Concentration measurements, however, are available at an asynchronous sampling rate. This model is also of interest for systems controlled through a hybrid communication network in which wireless sensors are used to add redundancy to existing working control loops (which use point-to-point wired communication links and continuous measurements) because wireless communication is often subject to data losses due to interference.

If there exists a nonzero probability that the system operates in open loop for a period of time large enough for the state to leave the stability region or even diverge to infinity (i.e., finite escape time), it is not possible to provide guaranteed stability properties. In order to study the stability properties in a deterministic framework, in this paper we consider systems where there is a limit on the maximum number of consecutive sampling times in which measurements of x_i, $i = n_s ... n_s + n_a$, are not available, i.e.

$$\max(t_{k+1,i} - t_{k,i}) \leq \Delta_M$$

This bound on the maximum period of time in which the loop is open has been also used in other works in the literature[25,38−41] and allows us to study deterministic notions of stability.

2.3. Asynchronous State Observer. An observer that takes advantage of synchronous measurements, asynchronous measurements, and a process model can be constructed to estimate the fault-free evolution of asynchronous states between consecutive measurements. The observer states are updated by setting the observer state equal to the measurement each time a new asynchronous measurement becomes available, $t_{k,i}$. The asynchronous state observer takes the form

$$\begin{aligned}
\dot{\hat{x}}_{n_s+1} &= f_{n_s+1}(x_1, ..., x_{n_s}, \hat{x}_{n_s+1}, ..., \hat{x}_{n_s+n_a}, u, 0, ..., 0)\\
&\vdots\\
\dot{\hat{x}}_{n_s+n_a} &= f_{n_s+n_a}(x_1, ..., x_{n_s}, \hat{x}_{n_s+1}, ..., \hat{x}_{n_s+n_a}, u, 0, ..., 0)
\end{aligned} \tag{3}$$

with $\hat{x}_i(t_{k,i}) = x_i(t_{k,i})$ for all $t_{k,i}$; that is, each time a new asynchronous measurement is received, the estimated states $\hat{x}_i$ with $i = n_s + 1, ..., n_s + n_a$ are reset to match the true process state. The information generated by this observer provides a fault-free estimate for each asynchronous state at any time t and allows for the design of nonlinear control laws that utilize

full state information. Using the estimated states, the control input applied to the system is given by

$$u = h(\hat{x}) \tag{4}$$

with

$$\hat{x} = \begin{bmatrix} x_1 \\ \vdots \\ x_{n_s} \\ \hat{x}_{n_s+1} \\ \vdots \\ \hat{x}_{n_s+n_a} \end{bmatrix} \in R^{n_s+n_a}$$

This control input is defined for all times because it is based on both the synchronous states and the estimated asynchronous states. We assume that Δ_M is small enough to guarantee that the system in closed loop with this control scheme is practically stable; see refs 25 and 38−41 for details on similar stability results.

2.4. Design of Fault Detection and Isolation Filter. Fault-tolerant control methods rely on the availability of a fall-back configuration that can maintain system stability and a control supervisor that will orchestrate the mode transition in a timely manner. The stability of the fault-tolerant control system depends on accurate and timely FDI, stability of the closed-loop system under the fall-back configuration, and the location of the state in the state space upon FDI and reconfiguration. In this section we construct fault detection and isolation (FDI) filters that will automatically identify the source of a failure in a timely manner. Utilizing synchronous state measurements, $x_i(t)$ with $i = 1, ..., n_s$ and asynchronous state estimates, $\hat{x}_i(t)$ with $i = n_s + 1, ..., n_s + n_a$, the following $n_s + n_a$ filters (one for each state in x) are defined:[21]

$$\dot{\tilde{x}}_i = f_i(x_1, ..., \tilde{x}_i, ..., x_{n_s}, \hat{x}_{n_s+1}, ..., \hat{x}_{n_s+n_a}, u_i, 0, ..., 0), \quad i = 1, ..., n_s$$

$$u_i = h(x_1, ..., \tilde{x}_i, ..., x_{n_s}, \hat{x}_{n_s+1}, ..., \hat{x}_{n_s+n_a}), \quad i = 1, ..., n_s$$

$$\dot{\tilde{x}}_i = f_i(x_1, ..., x_{n_s}, \hat{x}_{n_s+1}, ..., \tilde{x}_i, ..., \hat{x}_{n_s+n_a}, u_i, 0, ..., 0), \quad i = n_s + 1, ..., n_s + n_a$$

$$u_i = h(x_1, ..., x_{n_s}, \hat{x}_{n_s+1}, ..., \tilde{x}_i, ..., \hat{x}_{n_s+n_a}), \quad i = n_s + 1, ..., n_s + n_a \tag{5}$$

where $\tilde{x}_i$ is the filter output for the ith state. The FDI filters are only initialized at $t = 0$ such that $\tilde{x}_i(0) = x_i(0)$, $i = 1, ..., n_s + n_a$. For each state, the FDI residual can be defined as

$$r_i(t) = |x_i(t) - \tilde{x}_i(t)|, \quad i = 1, ..., n_s + n_a$$

The synchronous residuals $r_i(t)$ with $i = 1, ..., n_s$ are computed continuously because $x_i(t)$ with $i = 1, ..., n_s$ is known for all t. On the other hand, the asynchronous residuals $r_i(t)$ with $i = n_s + 1, ..., n_s + n_a$ are computed only at times $t_{k,i}$ when a new asynchronous measurement of $x_i(t)$ with $i = n_s, ..., n_s + n_a$ is received. These FDI filters operate by essentially predicting the fault-free evolution of each individual state, accounting for faults that enter the system when the predicted evolution of the state diverges from the measured evolution.[21]

The dynamics of both the asynchronous observers, $\hat{x}_i$, and the FDI filters, $\tilde{x}_i$, are identical to those of (1) when there are no disturbances or noise acting on the system. When the states are initialized as $\hat{x}_i(0) = \tilde{x}_i(0) = x_i(0)$ both the observer and filter states will track the true process states. For the synchronous case when a fault, d_i, occurs, only the corresponding residual, r_i, will become nonzero. This is the case when the f_i with $i = 1, ..., n_s$ vector field has a structure such that type I faults are isolable; see ref 21 for a precise determination of such a structure. In the case with asynchronous measurements, at least one r_i will become nonzero when a fault occurs. However, faults that affect asynchronous states may cause the asynchronous observer $\hat{x}_i$ to diverge from the true process state x_i between consecutive measurements, and any FDI filter states that are a function of $\hat{x}_i$ will no longer accurately track the corresponding true process states. When such a fault occurs, more than one residual value may become nonzero. In general, for fault isolation purposes, we assume that only one fault is affecting the system at any given time. While it may be possible in some circumstances to discriminate multiple faults, we do not consider this situation in the present work.

Continuous measurements for asynchronous states are not available, thus the FDI filters of (5) cannot always completely isolate all failures. We consider two classes of faults. Type I faults are faults that only affect states that are measured continuously; that is, d_j is a type I fault if

$$\frac{\partial f_i}{\partial d_j} = 0, \quad \forall i = n_s + 1, ..., n_s + n_a$$

Type II faults affect at least one asynchronous state; that is, d_j is a type II fault if there exists at least one $i = n_s + 1, ..., n_s + n_a$ such that

$$\frac{\partial f_i}{\partial d_j} \neq 0$$

The FDI filter will detect and isolate a type I fault d_j because the asynchronous state observers will track the asynchronous states accurately (i.e., the effect of the fault $d_j(t)$ on an asynchronous observer state is accounted for through the synchronous states, so $d_j(t)$ is accounted for in the observer (3) and hence the FDI filter). A type II fault enters the system in the differential equation of a state that is sampled asynchronously. The effect of type II faults cannot be accounted for by the observer $\hat{x}_i$, and such a fault will cause $\hat{x}_i$ to no longer track x_i and will eventually affect other coupled filter states as well. Strict isolation cannot take place for a type II fault. The FDI filter will detect and partially isolate disturbances in this case because the asynchronous state observers will diverge from the asynchronous states (i.e., the effect of the fault $d_j(t)$ on an asynchronous observer state is unmeasured and unaccounted for; thus (3) does not track the disturbed state). In other words, if a type I fault occurs, then it can be detected and isolated. If a type II fault occurs, then this fault can be grouped to the subset of type II faults.

A fault is detected at time t_f if there exists a residual i such that $r_i(t_f) > r_{i,\max}$, where $r_{i,\max}$ is an appropriate threshold that can be chosen to account for process and sensor noise and allow for normal process variation. In order to isolate the possible source of the fault, it is necessary to wait until the residuals of all the asynchronous state filters are updated after t_f to determine if the fault is type I or type II. The residual of each asynchronous state filter $\tilde{x}_i$ is updated at time

$$t_i(t_f) = \min_k t_{k,i} | t_{k,i} > t_f$$

If $r_i(t_i(t_f)) \leq r_{i,\max}$ with $i = n_s + 1, ..., n_s + n_a$, then the fault occurred at time t_f is a type I fault and can be appropriately isolated. Otherwise, the fault belongs to the set of type II faults.

Table 1. Polyethylene Reactor Noise Parameters

	σ_p	σ_m	ϕ
[In]	1×10^{-4}	5×10^{-2}	0
[M_1]	1×10^{-4}	5×10^{-2}	0.7
Y	1×10^{-4}	1×10^{-2}	0.7
T	5×10^{-3}	5×10^{-2}	0.7
T_{g1}	5×10^{-3}	5×10^{-2}	0.7
T_{w1}	5×10^{-3}	5×10^{-2}	0.7

Consider that a synchronous residual r_i indicates a fault at time t_f. In this case the fault could have two possible causes, a type I or type II fault. In order to determine the true cause of this fault, one has to wait for the complete set of asynchronous measurements to arrive after t_f. When all the asynchronous measurements arrive and if all the residuals of the asynchronous states are smaller than the threshold, then the fault can be attributed to a type I fault. If any asynchronous measurement arrives and the corresponding residual indicates a fault, then the fault is type II. Note that when an asynchronous residual indicates a fault, we can also conclude that the fault is type II. When the fault is type II, it has been detected, and it is possible to narrow the fault source down to the set of faults that enter the differential equations of asynchronous states.

When the fault can be attributed to a type I fault and it has been detected and isolated, then automated fault tolerant control (FTC) action can be initiated. For example, when a fault event that is due to a manipulated input failure (i.e., an actuator failure) is detected and isolated, fault-tolerant control methods can be initiated.[21] In general, an FTC switching rule may be employed that orchestrates the reconfiguration of the control system in the event of control system failure. This rule determines which of the backup control loops can be activated, in the event that the main control loop fails, in order to preserve closed-loop stability. Owing to the limitations imposed by input constraints on the stability region for each control configuration, switching from a malfunctioning configuration to a well-functioning, but randomly selected, backup configuration will not preserve closed-loop stability if the state of the system, at the time of failure, lies outside the stability region of the chosen backup configuration. In this case, stabilization using this configuration requires more control action than is allowed by its constraints. This observation motivates the development of switching logic, which is to switch to the control configuration for which the closed-loop state resides within the stability region at the time of control failure. Without loss of generality, let the initial actuator configuration be $k(0) = 1$ and let t_d be the time when this failure has been isolated, then the switching rule given by

$$k(t) = j \; \forall \; t \geq t_d \qquad \text{if } x(t_d) \in \Omega(u_j^{\max}) \tag{6}$$

for some $j \in \{2, 3, ..., N\}$ guarantees closed-loop asymptotic stability, where $\Omega(u_j^{\max})$ is the stability region for the jth control configuration. The implementation of the above switching law requires monitoring the closed-loop state trajectory with respect to the stability regions associated with the various fall-back configurations. The reader may refer to ref 34 for application of FTC to a polyethylene reactor with constraints on the manipulated inputs. In this work we consider a control law without constraints on the manipulated inputs, and the primary control configuration with a faulty actuator will be deactivated in favor of a fully functional fall-back control configuration where the fall-back configuration can guarantee global stability of the closed-loop system. This integrated FDI/FTC reconfiguration allows for seamless fault recovery in the event of an actuator failure. Section 3 demonstrates integrated FDI/FTC for the polyethylene reactor.

Remark 2. In the process model of (1), process and sensor noise are not explicitly taken into account. However, noise is indirectly accounted for in the FDI method below by means of appropriate tolerance thresholds in the decision criteria for fault detection and isolation, that is, $r_{i,\max}$. The thresholds are generated on the basis of operating data and take into account both sensor and process noise, allowing for an appropriate FDI performance even if the process model and the measurements are corrupted by noise. To demonstrate this point, process and sensor noise are included in the simulation study; see section 3 for details. Note that the proper selection of the fault detection thresholds can account for some plant-model mismatch. However, a reasonably accurate model of the plant is generally required as excessive plant-model mismatch can lead to inaccurate FDI.

Remark 3. In this work, we consider all states to be measured, either synchronously or asynchronously. In general, it is possible that some states may be entirely unmeasurable, requiring the use of state estimators or observers to estimate them. We also assume that there is not time delay in the asynchronous readings. Although it may be possible for asynchronous measurements to be delayed, this does not present a problem as long as the delay is known. In such a case, the filters and observers should be integrated from the actual measurement time.

3. Application to a Polyethylene Reactor with Asynchronous Measurements

3.1. Process and Measurement Modeling. The proposed model based asynchronous FDI and FTC method will be demonstrated using a model of an industrial gas phase polyethylene reactor. The feed to the reactor consists of ethylene, comonomer, hydrogen, inerts, and catalyst. A recycle stream of unreacted gases flows from the top of the reactor and is cooled by passing through a water-cooled heat exchanger. Cooling rates in the heat exchanger are adjusted by mixing cold and warm water streams while maintaining a constant total cooling water flow rate through the heat exchanger. Mass balances on hydrogen and comonomer have not been considered in this study because hydrogen and comonomer have only mild effects on the reactor dynamics.[33] A mathematical model for this reactor has the following form:[42]

$$\frac{\mathrm{d[In]}}{\mathrm{d}t} = \frac{1}{V_g}\left(F_{\mathrm{In}} - \frac{[\mathrm{In}]}{[\mathrm{M_1}] + [\mathrm{In}]} b_t\right)$$

$$\frac{\mathrm{d[M_1]}}{\mathrm{d}t} = \frac{1}{V_g}\left(F_{M_1} - \frac{[\mathrm{M_1}]}{[\mathrm{M_1}] + [\mathrm{In}]} b_t - R_{M_1}\right) + d_4$$

$$\frac{\mathrm{d}Y_1}{\mathrm{d}t} = F_c a_c - k_{d_1} Y_1 - \frac{R_{M_1} M_{W_1} Y_1}{B_w} + d_2$$

$$\frac{\mathrm{d}Y_2}{\mathrm{d}t} = F_c a_c - k_{d_2} Y_2 - \frac{R_{M_1} M_{W_1} Y_2}{B_w} + d_2$$

$$\frac{\mathrm{d}T}{\mathrm{d}t} = \frac{H_f + H_{g1} - H_{g0} - H_r - H_{\mathrm{pol}}}{M_r C_{pr} + B_w C_{\mathrm{ppol}}} + Q + d_1$$

$$\frac{\mathrm{d}T_{w_1}}{\mathrm{d}t} = \frac{F_w}{M_w}(T_{wi} - T_{w_1}) - \frac{UA}{M_w C_{pw}}(T_{w_1} - T_{g_1})$$

$$\frac{\mathrm{d}T_{g_1}}{\mathrm{d}t} = \frac{F_g}{M_g}(T - T_{g_1}) + \frac{UA}{M_g C_{pg}}(T_{w_1} - T_{g_1}) + d_3 \tag{7}$$

where

$$b_t = V_p C_v \sqrt{([\mathrm{M}_1] + [\mathrm{In}])RRT - P_v}$$

$$R_{M_1} = [\mathrm{M}_1] k_{p0} \exp\left[-\frac{E_a}{R}\left(\frac{1}{T} - \frac{1}{T_f}\right)\right](Y_1 + Y_2)$$

$$C_{pg} = \frac{[\mathrm{M}_1]}{[\mathrm{M}_1] + [\mathrm{In}]} C_{pm1} + \frac{[\mathrm{In}]}{[\mathrm{M}_1] + [\mathrm{In}]} C_{p\mathrm{In}}$$

$$H_f = (F_{M_1} C_{pm1} + F_{\mathrm{In}} C_{p\mathrm{In}})(T_{\mathrm{feed}} - T_f)$$

$$H_{g1} = F_g(T_{g_1} - T_f) C_{pg}$$

$$H_{g0} = (F_g + b_t)(T - T_f) C_{pg}$$

$$H_r = H_{\mathrm{reac}} M_{W_1} R_{M_1}$$

$$H_{\mathrm{pol}} = C_{\mathrm{ppol}}(T - T_f) R_{M_1} M_{W_1} \qquad (8)$$

The definitions for all the variables used in (7) and (8) are given in Table 2, and their values can be found in ref 42 (see also ref 34). Under normal operating conditions, the open-loop system behaves in an oscillatory fashion (i.e., the system possesses an open-loop unstable steady state surrounded by a stable limit cycle). The open-loop unstable steady state around which the system will be controlled is

$$[\mathrm{In}]_{ss} = 439.7 \text{ mol/m}^3 \quad [\mathrm{M}_1]_{ss} = 326.7 \text{ mol/m}^3$$
$$Y_{1ss}, Y_{2ss} = 3.835 \text{ mol} \quad T_{ss} = 356.2 \text{ K}$$
$$T_{g1ss} = 290.4 \text{ K} \quad T_{w1ss} = 294.4 \text{ K}$$

Note that with the given parameters the dynamics of Y_1 and Y_2 are identical and will be reported in the results as a single combined state. In this example, we consider four possible faults, d_1, d_2, d_3, and d_4, which represent a heat jacket fault, catalyst deactivation, a change in the recycle gas flow rate, and ethylene consumption, respectively. The primary manipulated input for these studies is the heat input, Q, and the fall-back manipulated input is the feed temperature, T_{feed}. In practice, the temperature of the feed stream would be manipulated via a heat exchanger positioned on the feed line before it enters the process. A fall-back manipulated input is required to maintain desired system performance in the presence of failure in the primary control configuration.

Simulations have been carried out for several scenarios to demonstrate the effectiveness of the proposed FDI scheme in detecting and isolating the four faults d_1, d_2, d_3, and d_4 in the presence of asynchronous measurements. The temperature measurements (T, T_{g1}, T_{w1}) are all assumed to be available synchronously, while the concentration measurements ([In], [M_1], Y) arrive at asynchronous intervals. In all the simulations, sensor measurement and process noise are included. The sensor measurement noise trajectory was generated using a sample time of 10 s and a zero-mean normal distribution with standard deviation σ_M. The autoregressive process noise was generated discretely as $w_k = \phi w_{k-1} + \xi_k$, where $k = 0, 1, \ldots$ is the discrete time step, with a sample time of 10 s, ϕ is the autoregressive coefficient, and ξ_k is obtained at each sampling step using a zero-mean normal distribution with standard deviation σ_p. The autoregressive process noise is added to the right-hand side of the differential equations for each state, and the sensor measurement noise is added to the measurements of each state. Sensor measurement noise and process noise are evaluated independently for each state variable. The process and sensor measurement noise for Y_1 and Y_2 are taken to be equal. Table 1 provides the values of the noise parameters for each state of system (7). The length of time between consecutive asynchronous measurements is

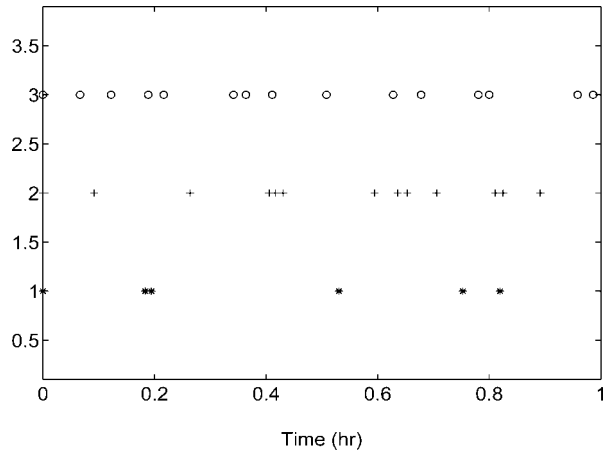

Figure 1. Asynchronous sampling times $t_{k,[\mathrm{In}]}$ (star), $t_{k,[\mathrm{M}_1]}$ (cross), and $t_{k,Y}$ (circle) with a fault d_1 at $t = 0.5$ h.

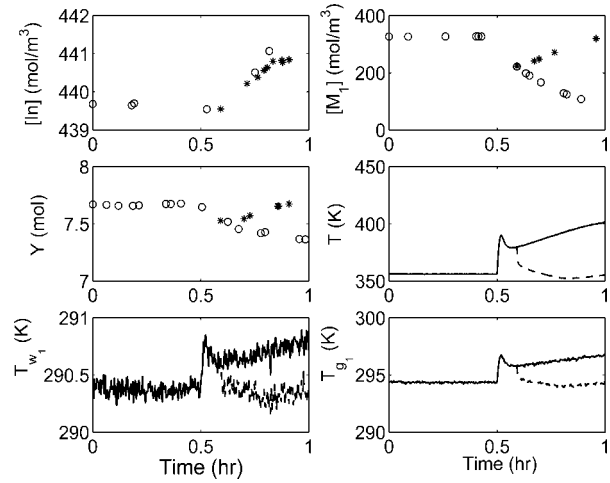

Figure 2. State trajectories of the closed-loop system without fault-tolerant control (circle/solid) and with appropriate fault-detection and isolation and fault-tolerant control where the fall-back control configuration is activated (star/dotted) with a fault d_1 at $t = 0.5$ h.

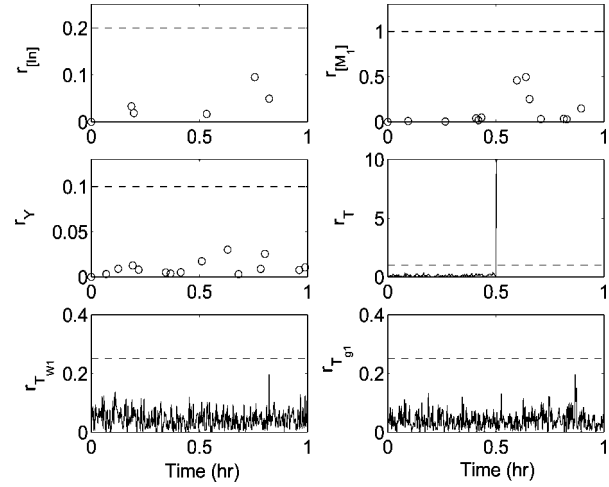

Figure 3. Fault detection and isolation residuals for the closed-loop system with a fault d_1 at $t = 0.5$ h. The fault is detected immediately, but isolation occurs at $t = 0.59$ h when all three asynchronous states have reported a residual below their detection threshold. This signals a type I fault, and we can isolate the source of this fault as d_1.

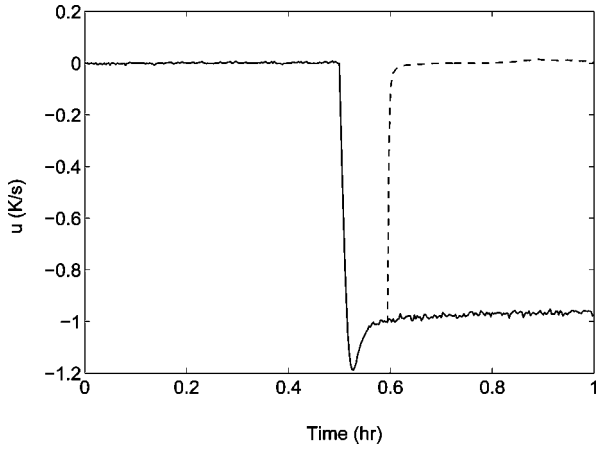

Figure 4. Manipulated input for the closed-loop system without fault-tolerant control (solid) and with appropriate fault-tolerant control where the fall-back control configuration is activated (dotted) with a fault d_1 at $t = 0.5$ h.

generated randomly based on a Poisson process. The time when the system will receive the next ith asynchronous measurement is given by $t_{k+1,i} = t_{k,i} + \Delta_a$, where $\Delta_a = \ln(\xi)/W_a$ and $\xi \in (0, 1)$ is a random variable chosen from a uniform probability distribution and $W_a = 0.003\ \mathrm{s}^{-1}$ is the mean rate of asynchronous sampling. There is an upper bound limiting the time between consecutive measurements such that $\Delta_a \leq \Delta_M = 1200$ s. This value of Δ_M is small enough to provide practical closed-loop stability around the desired equilibrium point for the polyethylene reactor of (7). An increasing sequence of measurement arrival times is generated independently for each asynchronously measured state.

3.2. Design of the asynchronous state observers. To perform FDI for the polyethylene reactor system, we need to construct the asynchronous state observers of (3). The asynchronous state observers for this system have the following form:

$$\frac{\mathrm{d}[\hat{\mathrm{In}}]}{\mathrm{d}t} = \frac{1}{V_g}\left(F_{\mathrm{In}} - \frac{[\hat{\mathrm{In}}]}{[\hat{\mathrm{M}}_1] + [\hat{\mathrm{In}}]}\hat{b}_t\right)$$

$$\frac{\mathrm{d}[\hat{\mathrm{M}}_1]}{\mathrm{d}t} = \frac{1}{V_g}\left(F_{M_1} - \frac{[\hat{\mathrm{M}}_1]}{[\hat{\mathrm{M}}_1] + [\hat{\mathrm{In}}]}\hat{b}_t - \hat{R}_{M_1}\right)$$

$$\frac{\mathrm{d}\hat{Y}}{\mathrm{d}t} = F_c a_c - k_{d_1}\hat{Y} - \frac{\hat{R}_{M_1} M_{W_1}\hat{Y}}{B_w}$$

$$\hat{b}_t = V_p C_v \sqrt{([\hat{\mathrm{M}}_1] + [\hat{\mathrm{In}}])RRT(t) - P_v}$$

$$\hat{R}_{M_1} = [\hat{\mathrm{M}}_1] k_{p0} \exp\left[\left(-\frac{E_a}{R}\right)\left(\frac{1}{T(t)} - \frac{1}{T_f}\right)\right](\hat{Y})$$

$$[\hat{\mathrm{In}}](t_{k,[\mathrm{In}]}) = [\mathrm{In}](t_{k,[\mathrm{In}]})$$

$$[\hat{\mathrm{M}}_1](t_{k,[\mathrm{M}_1]}) = [\mathrm{M}_1](t_{k,[\mathrm{M}_1]})$$

$$\hat{Y}(t_{k,Y}) = Y(t_{k,Y}) \tag{9}$$

where $[\hat{\mathrm{In}}]$, $[\hat{\mathrm{M}}_1]$, and $\hat{Y}$ are the asynchronous observer states. Each asynchronous observer state is initialized each time new measurement information becomes available at the times $t_{k,i}$. The observer states provide estimates for the asynchronous states between consecutive measurements allowing the computation of control actions and FDI residuals at each time.

3.3. Design of the State Feedback Controller. The control objective is to stabilize the system at the open-loop unstable steady state. A nonlinear Lyapunov-based feedback controller that enforces asymptotic stability of the closed-loop system is synthesized using the method proposed in ref 37 (see also ref 43). This is a single input controller that utilizes synchronous measurements as well as observer states generated by (9). System (7) belongs to the following class of nonlinear systems

$$\dot{x}(t) = f(x(t)) + g_1(x(t))u_1(t) + g_2(x(t))u_2(t) + w(x(t))d(t) \tag{10}$$

where

$$x(t) = \begin{bmatrix} [\mathrm{In}] - [\mathrm{In}]_{ss} \\ [\mathrm{M}_1] - [\mathrm{M}_1]_{ss} \\ Y - Y_{ss} \\ T - T_{ss} \\ T_{g1} - T_{g1ss} \\ T_{w1} - T_{w1ss} \end{bmatrix}$$

and

$$u_1(t) = Q, \quad u_2(t) = T_{\mathrm{feed}}$$

Consider the quadratic control Lyapunov function $V(x) = x^{\mathrm{T}}\mathbf{P}x$ where

$$\mathbf{P} = 1 \times 10^{-2}\ \mathrm{diag}[0.5\ 0.5\ 0.51\ 0.005\ 0.005]$$

The values of the weighting matrix $\mathbf{P}$ are chosen to account for the different range of numerical values for each state. The following feedback laws[37] asymptotically stabilize the open loop and possibly unstable steady state of the nominal system (i.e., $d(t) \equiv 0$)

$$h_i(x) = \begin{cases} -\dfrac{L_f V + \sqrt{L_f V^2 + L g_i V^4}}{L_{g_i} V} & \text{if } L_{g_i} V \neq 0 \\ 0 & \text{if } L_{g_i} V = 0 \end{cases}, \quad i = 1, 2 \tag{11}$$

where $L_f V$ and $L_{g_i} V$ denote the Lie derivatives of the scalar function V with respect to the vectors fields f and g_i, respectively.

In the simulations, the primary control configuration is given by

$$u_1(t) = h_1(\hat{x}(t))$$

and the fall-back control configuration is given by

$$u_2(t) = h_2(\hat{x}(t))$$

where

$$\hat{x}(t) = \begin{bmatrix} [\hat{\mathrm{In}}] - [\mathrm{In}]_{ss} \\ [\hat{\mathrm{M}}_1] - [\mathrm{M}_1]_{ss} \\ \hat{Y} - Y_{ss} \\ T - T_{ss} \\ T_{g1} - T_{g1ss} \\ T_{w1} - T_{w1ss} \end{bmatrix}$$

3.4. Design of FDI/FTC Scheme. Fault detection and isolation for the system in closed loop with the primary configuration is accomplished by generating FDI filters from (5), and for the polyethylene system the FDI filters take the following form:

$$\frac{d[\tilde{I}n]}{dt} = \frac{1}{V_g}\left(F_{In} - \frac{[\tilde{I}n]}{[\hat{M}_1] + [\tilde{I}n]}\tilde{b}_t^{[In]}\right)$$

$$\frac{d[\tilde{M}_1]}{dt} = \frac{1}{V_g}\left(F_{M_1} - \frac{[\tilde{M}_1]}{[\tilde{M}_1] + [\hat{I}n]}\tilde{b}_t^{[M_1]} - \tilde{R}_{M_1}^{[M_1]}\right)$$

$$\frac{d\tilde{Y}}{dt} = F_c a_c - k_{d_1}\tilde{Y} - \frac{\tilde{R}_{M_1}^{Y} M_{W_1}\tilde{Y}}{B_w}$$

$$\frac{d\tilde{T}}{dt} = \frac{H_f + \tilde{H}_{g1}^T - \tilde{H}_{g0}^T - \tilde{H}_r^T - \tilde{H}_{pol}^T}{M_r C_{pr} + B_w C_{ppol}} + h_1(\hat{x}(t))$$

$$\frac{d\tilde{T}_{w_1}}{dt} = \frac{F_w}{M_w}(T_{wi} - \tilde{T}_{w_1}) - \frac{UA}{M_w C_{pw}}(\tilde{T}_{w_1} - T_{g_1})$$

$$\frac{d\tilde{T}_{g_1}}{dt} = \frac{F_g}{M_g}(T - \tilde{T}_{g_1}) + \frac{UA}{M_g \tilde{C}_{pg}}(T_{w_1} - \tilde{T}_{g_1}) \quad (12)$$

where

$$\begin{aligned}
\tilde{b}_t^{[In]} &= V_p C_v \sqrt{([\hat{M}_1] + [\tilde{I}n])RRT - P_v} \\
\tilde{b}_t^{[M_1]} &= V_p C_v \sqrt{([\tilde{M}_1] + [\hat{I}n])RRT - P_v} \\
\tilde{b}_t^{[T]} &= V_p C_v \sqrt{([\hat{M}_1] + [\hat{I}n])RR\tilde{T} - P_v} \\
\tilde{R}_{M1}^{[M_1]} &= [\tilde{M}_1] k_{p0} \exp\left[-\frac{E_a}{R}\left(\frac{1}{T} - \frac{1}{T_f}\right)\right](\hat{Y}) \\
\tilde{R}_{M1}^{Y} &= [\hat{M}_1] k_{p0} \exp\left[-\frac{E_a}{R}\left(\frac{1}{T} - \frac{1}{T_f}\right)\right](\tilde{Y}) \\
\tilde{R}_{M1}^{T} &= [\hat{M}_1] k_{p0} \exp\left[-\frac{E_a}{R}\left(\frac{1}{\tilde{T}} - \frac{1}{T_f}\right)\right](\hat{Y}) \\
\tilde{C}_{pg} &= \frac{[\hat{M}_1]}{[\hat{M}_1] + [\hat{I}n]} C_{pm1} + \frac{[\hat{I}n]}{[\hat{M}_1] + [\hat{I}n]} C_{pIn} \\
\tilde{H}_{g1}^T &= F_g(T_{g_1} - T_f)\tilde{C}_{pg} \\
\tilde{H}_{g0}^T &= (F_g + \tilde{b}_t^T)(\tilde{T} - T_f)\tilde{C}_{pg} \\
\tilde{H}_r^T &= H_{reac} M_{W_1} \tilde{R}_{M_1}^T \\
\tilde{H}_{pol}^T &= C_{ppol}(\tilde{T} - T_f)\tilde{R}_{M_1}^T M_{W_1}
\end{aligned} \quad (13)$$

In addition, the FDI residuals take the following form:

$$\begin{aligned}
r_{[In]} &= |[In](t_k) - [\tilde{I}n](t_k)| \\
r_{[M_1]} &= |[M_1](t_k) - [\tilde{I}n](t_k)| \\
r_Y &= |Y(t_k) - \tilde{Y}(t_k)| \\
r_T &= |T - \tilde{T}| \\
r_{T_{g_1}} &= |T_{g_1} - \tilde{T}_{g_1}| \\
r_{T_{w_1}} &= |T_{w_1} - \tilde{T}_{w_1}|
\end{aligned} \quad (14)$$

In the case with measurement and process noise, the residuals will be nonzero even without a failure event. This motivates the use of detection thresholds such that a fault is declared when a residual exceeds a specific threshold value, $r_{i,max}$ (note that a different threshold value can be used for each residual, see remark 2). This threshold value must be selected to avoid false alarms due to process and measurement noise, but it should also be sensitive enough (small enough) to detect faults in a timely manner so that efficient FTC action can be initiated. The threshold values used for each residual in the numerical simulations can be seen as the dashed lines in Figures 3, 7, 11, and 15.

If the fault can be isolated to d_1 (i.e., r_T exceeds $r_{T,max}$ at $t = t_f$, while $r_i(t_i(t_f)) \leq r_{i,max}$ with $i = [In], [M_1], Y$), then one can invoke fault tolerant control methods to handle actuator failures by activation of a fall-back control configuration. In the simulation studies, it is assumed that a fall-back configuration, where the fall-back manipulated input $u_2 = T_{feed}$, is available. The control law of (11) enforces stability when the control actuator is functioning properly; thus switching to the operational fall-back configuration will guarantee stability in the case of failure of the primary control configuration, $u_1 = Q$.

3.5. Closed-Loop Process Simulation Results. This section consists of four simulation studies, each examining one of the faults d_1, d_2, d_3, or d_4 as shown in (7). The first simulation considers a fault, d_1, on the heating jacket which is the primary manipulated input. In this case the simulation includes fault-tolerant control that automatically reconfigures the plant so that the fall-back manipulated input, $u_2 = T_{feed}$, is activated to maintain stability. Specifically, the supervisory control element will deactivate the primary control configuration, u_1 and activate the fall-back configuration u_2 when $r_T > r_{T,max}$ and $r_i(t_i(t_f)) \leq r_{i,max}$ with $i = [In]$, $[M_1]$, and Y. This specific fault signature corresponds to a type I fault that can be isolated to d_1. The reader may refer to ref 34 to obtain more information on FTC and reconfiguration rules for a polyethylene reactor with constraints on the manipulated inputs that give rise to stability regions. This work does not consider constraints on the manipulated inputs; hence, the fall-back configuration can guarantee stability from anywhere in the state space because the closed-loop system under the fall-back control configuration is globally asymptotically stable. The remaining simulation studies explore faults that disturb the system but do not arise from actuator failures. Since they are not caused by actuation component malfunctions, these failures cannot be resolved simply by actuator reconfiguration. However, these simulations demonstrate quick detection and isolation in the presence of asynchronous measurements that enables the operator to take appropriate and focused action in a timely manner.

For the fault d_1 a simulation study has been carried out to demonstrate the proposed asynchronous fault detection and isolation and fault tolerant control method. The sequence of asynchronous measurements for this scenario is shown in Figure 1. This first simulation uses the primary control configuration in which Q is the manipulated input and has a fall-back configuration, in which T_{feed} is the manipulated input, available in case of a fault in d_1. A fault takes place where $d_1 = 1$ K/s at $t = 0.5$ h representing a failure in the heating jacket, Q. At this time the synchronous states in Figure 2 all move away from the equilibrium point. Additionally, as asynchronous measurements become available, it is clear the asynchronous states also move away from the equilibrium point after the failure. It is unclear from the state information alone what caused this faulty behavior. However, if the FDI residuals in Figure 3 generated by (12) are examined, it is clear that the residual r_T that is associated with the manipulated input Q violates its threshold at $t_f = 0.5003$ h. The fault is detected upon this threshold violation. However, isolation cannot take place until one new measurement for each asynchronous state becomes available. At $t = 0.5944$ h all three required asynchronous measurements have arrived, and the asynchronous residuals remain below their thresholds; hence $r_i(t_i(t_f)) \leq r_{i,max}$ with $i = [In]$, $[M_1]$, and Y. This signals that this is a type I fault that can be isolated to d_1.

Table 2. Polyethylene Reactor Example Process Variables

a_c	active site concentration of catalyst
b_t	overhead gas bleed
B_w	mass of polymer in the fluidized bed
C_{pm1}	specific heat capacity of ethylene
C_v	vent flow coefficient
C_{pw}, $C_{p\text{In}}$, C_{ppol}	specific heat capacity of water, inert gas and polymer
E_a	activation energy
F_c, F_g	flow rate of catalyst and recycle gas
F_{In}, F_{M_1}, F_w	flow rate of inert, ethylene and cooling water
H_f, H_{g0}	enthalpy of fresh feed stream, total gas outflow stream from reactor
H_{g1}	enthalpy of cooled recycle gas stream to reactor
H_{pol}	enthalpy of polymer
H_r	heat liberated by polymerization reaction
H_{reac}	heat of reaction
[In]	molar concentration of inerts in the gas phase
k_{d1}, k_{d2}	deactivation rate constant for catalyst site 1, 2
k_{p0}	pre-exponential factor for polymer propagation rate
M_1	molar concentration of ethylene in the gas phase
M_g	mass holdup of gas stream in heat exchanger
M_rC_{pr}	product of mass and heat capacity of reactor walls
M_w	mass holdup of cooling water in heat exchanger
M_{W1}	molecular weight of monomer
P_v	pressure downstream of bleed vent
Q	heat added/removed by heating jacket
R, RR	ideal gas constant, unit of J/(mol K), (m^3 atm)/(mol K)
T, T_f, T_{feed}	reactor, reference, feed temperature
T_{g1}, T_{w1}	temperature of recycle gas, cooling water stream from exchanger
T_{wi}	inlet cooling water temperature to heat exchanger
UA	product of heat exchanger coefficient with area
V_g	volume of gas phase in the reactor
V_p	bleed stream valve position
Y_1, Y_2	moles of active site type 1, 2

At this time, the system is reconfigured to the fall-back configuration where T_{feed} is the manipulated input, and the resulting state trajectory, shown as the dotted line in Figure 2, moves back to the desired operating point. The manipulated input for this scenario can be seen in Figure 4 where the solid line is the manipulated input without detection and reconfiguration, and the dotted line represents the input after FDI and reconfiguration.

The second simulation demonstrates the proposed asynchronous model-based fault-detection and isolation method when a type II fault occurs. The sequence of asynchronous measurements for this scenario is shown in Figure 5. This simulation uses the primary control configuration in which Q is the manipulated input. A fault takes place where $d_2 = -0.001$ mol/s at $t = 0.5$ h representing a catalyst deactivation event. After the failure, two synchronous states in Figure 6 move away from the equilibrium point. Additionally, as asynchronous measurements become available it can be seen that asynchronous states also move away from the equilibrium point after the failure. It is unclear from the state information alone what caused this faulty behavior. However, if the FDI residuals in Figure 7 generated by (14) are examined, it is clear that the residuals $r_{[M_1]}$, r_Y, and r_T violate their thresholds. The fault is detected upon the first threshold violation (r_Y at $t = 0.5333$). When the residual associated with Y exceeds the threshold, this signals that the fault is type II and entered the system in the differential equation of an asynchronous state. When the fault is type II, it cannot be isolated. However, such a fault can be grouped in the subset of faults that enter into the differential equation of an asynchronous state, (i.e., the group of type II faults, specifically, d_2 or d_4). At this time, the system operator can utilize the above partial isolation to examine the plant and determine the exact source of the failure. The manipulated input for this scenario can be seen in Figure 8.

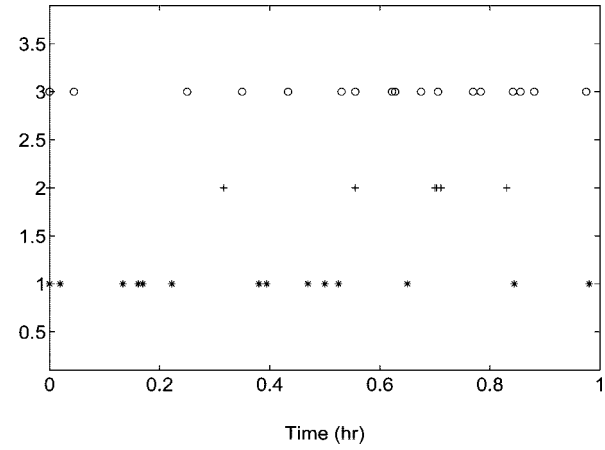

Figure 5. Asynchronous sampling times $t_{k,[\text{In}]}$ (star), $t_{k,[\text{M}_1]}$ (cross), and $t_{k,Y}$ (circle) with a fault d_2 at $t = 0.5$ h.

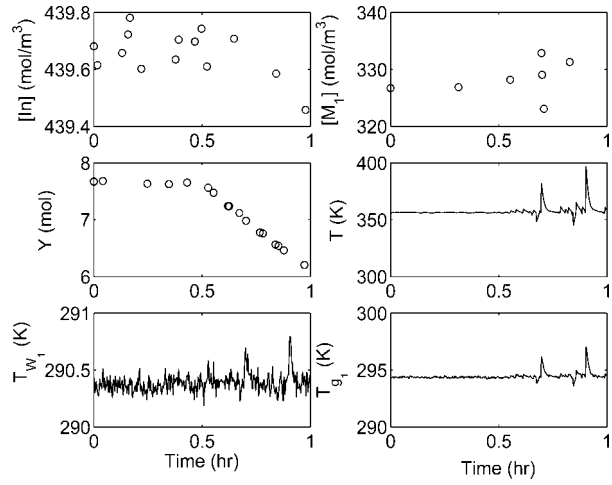

Figure 6. State trajectories of the closed-loop system with a fault d_2 at $t = 0.5$ h.

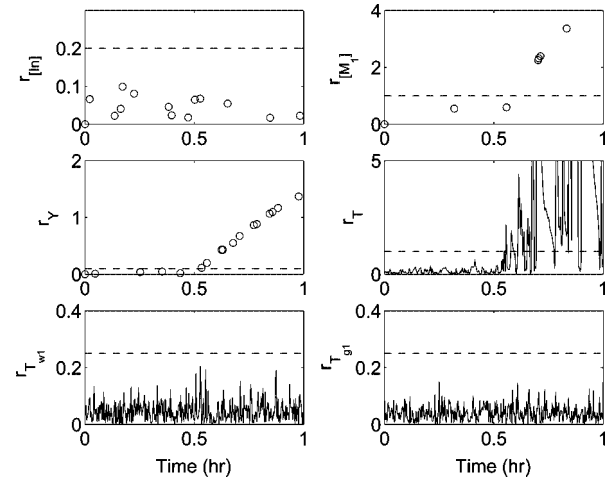

Figure 7. Fault detection and isolation residuals for the closed-loop system with a fault d_2 at $t = 0.5$ h. The fault is detected when residual for Y exceeds the threshold. Subsequently, T and [M_1] exceed their thresholds. When any asynchronous residual violates the threshold, this indicates that the fault is in the set of type II faults; d_2 or d_4.

The third simulation study examines FDI in the presence of a type I fault, d_3, representing a change in the recycle gas flow rate. The sequence of asynchronous measurements for this scenario is shown in Figure 9. This simulation study uses the

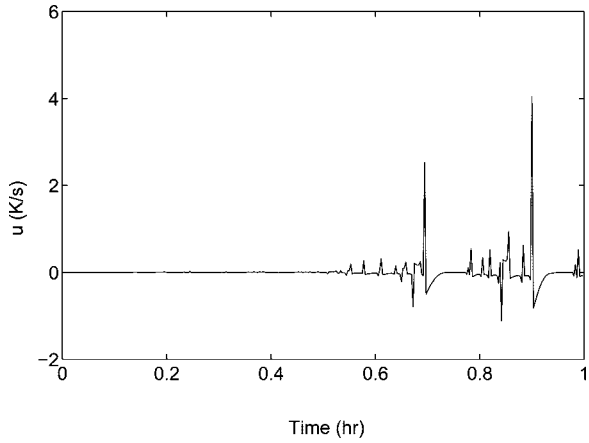

Figure 8. Manipulated input for the closed-loop system with a fault d_2 at $t = 0.5$ h.

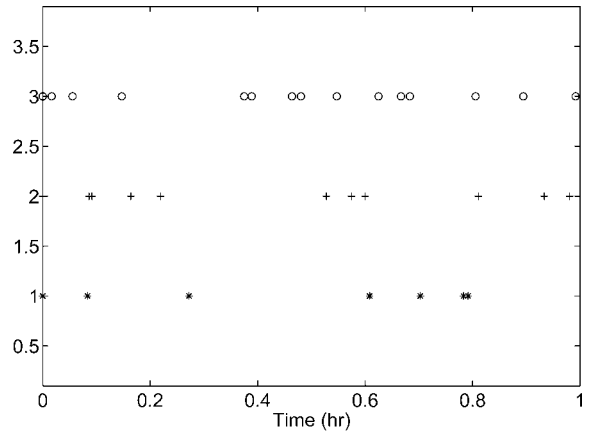

Figure 9. Asynchronous sampling times $t_{k,[\mathrm{In}]}$ (star), $t_{k,[\mathrm{M}_1]}$ (cross), and $t_{k,Y}$ (circle) with a fault d_3 at $t = 0.5$ h.

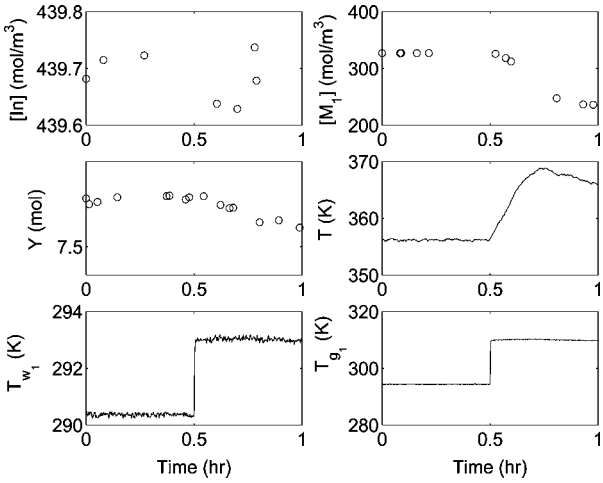

Figure 10. State trajectories of the closed-loop system with a fault d_3 at $t = 0.5$ h.

primary control configuration in which Q is the manipulate input, and a fault takes place where $d_3 = 300$ K/s at $t = 0.5$ h. At this time the synchronous states in Figure 10 all move away from the equilibrium point. Additionally, as asynchronous measurements become available it is observed that the asynchronous states also move away from the equilibrium point after the failure. It is unclear from the state information alone what caused this faulty behavior. However, if the FDI residuals in Figure 11 generated by (12), (13), and (14) are examined, the residual

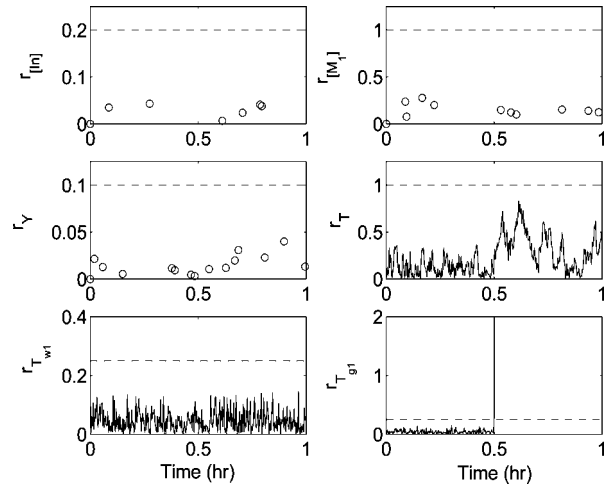

Figure 11. Fault detection and isolation residuals for the closed-loop system with a fault d_3 at $t = 0.5$ h. A fault is detected immediately when residual for T_{g1} exceeds the threshold. Subsequently, none of the asynchronous residuals exceed their thresholds, indicating that the fault source can be isolated as d_3.

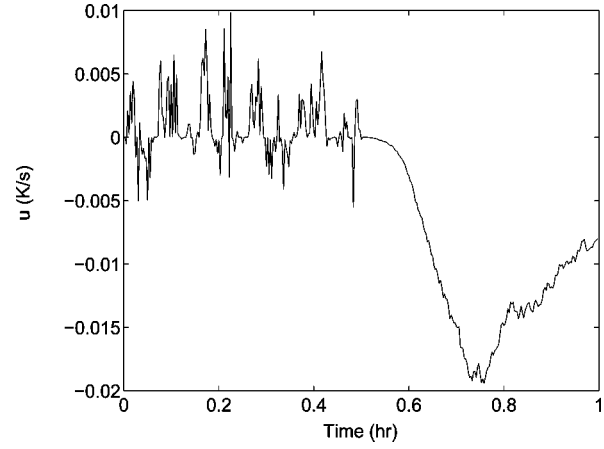

Figure 12. Manipulated input for the closed-loop system with a fault d_3 at $t = 0.5$ h.

associated with T_{g1} violates its threshold at $t = 0.5003$ h. The fault is detected upon this threshold violation. However, isolation cannot take place until one new measurement for each asynchronous state becomes available. At $t = 0.6086$ h all three required asynchronous measurements have become available, and the residuals signal a type I fault, allowing the isolation of the fault to d_3. The manipulated input for this scenario can be seen in Figure 12.

The final simulation study demonstrates the proposed asynchronous model-based fault detection and isolation method when a type II fault occurs. The sequence of asynchronous measurements for this scenario is shown in Figure 13. This simulation uses the primary control configuration in which Q is the manipulated input. A fault takes place where $d_4 = -0.2$ mol/s at $t = 0.5$ h representing unexpected monomer consumption. After the failure the synchronous states in Figure 14 diverge from their desired values. Additionally, as asynchronous measurements become available, it can be seen that asynchronous states also diverge after the failure. It is unclear from the state information alone what caused this faulty behavior. However, if the FDI residuals in Figure 15 generated by (12) are examined, the residuals $r_{[\mathrm{In}]}$, $r_{[\mathrm{M}_1]}$, r_T, and $r_{T_{g1}}$ violate their thresholds. The fault is detected upon the first threshold violation ($r_{[\mathrm{M}_1]}$ at $t = 0.05667$ h). When the residual $r_{[\mathrm{M}_1]}$ exceeds the

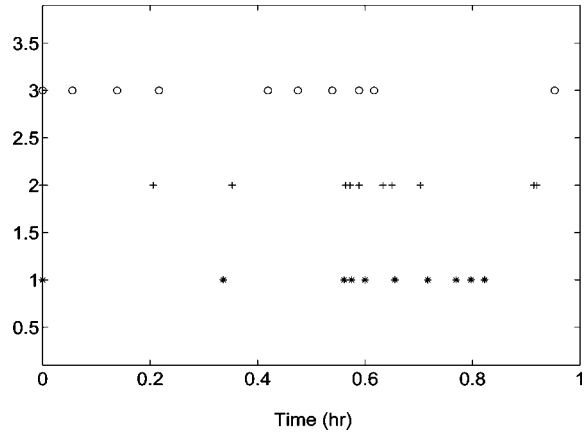

Figure 13. Asynchronous sampling times $t_{k,[In]}$ (star), $t_{k,[M_1]}$ (cross), and $t_{k,Y}$ (circle) with a fault d_4 at $t = 0.5$ h.

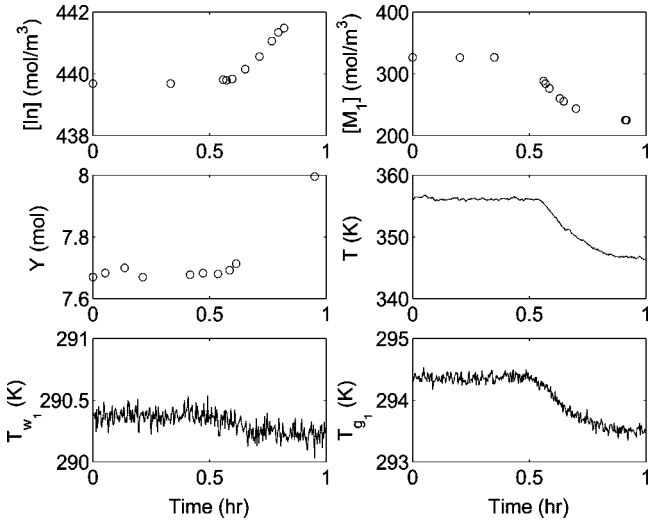

Figure 14. State trajectories of the closed-loop system with a fault d_4 at $t = 0.5$ h.

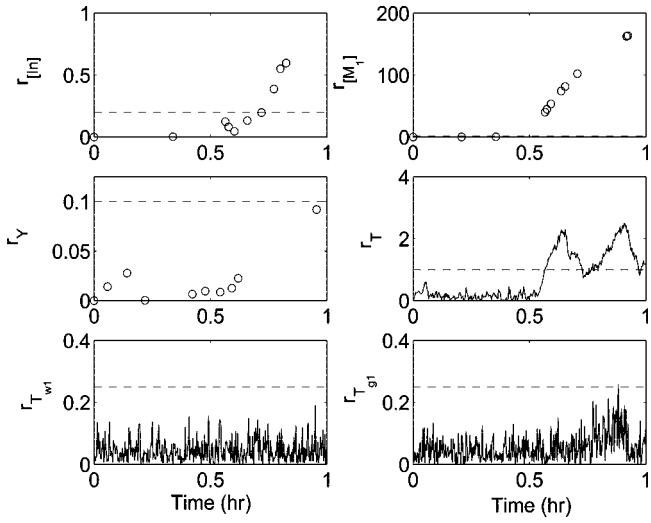

Figure 15. Fault detection and isolation residuals for the closed-loop system with a fault d_4 at $t = 0.5$ h. The fault is detected when residual for $[M_1]$ exceeds the threshold. Subsequently, T and [In] exceed their thresholds. When any asynchronous residual violates the threshold, this indicates the fault is in the set of type II faults; d_2 or d_4.

threshold, this signals that a type II fault has occurred. When a type II fault occurs, it cannot be isolated. As in the second simulation, such a fault can be grouped in the subset of type II

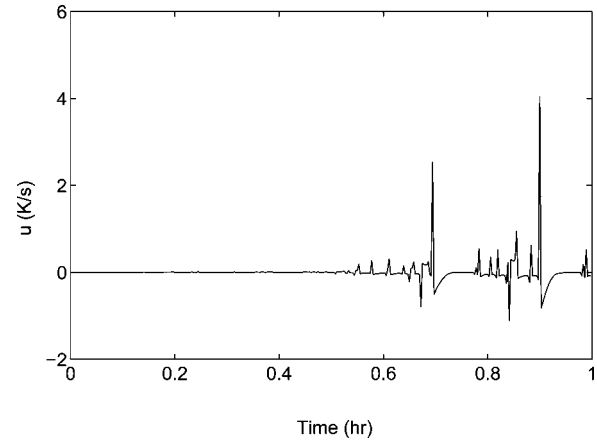

Figure 16. Manipulated input for the closed-loop system with a fault d_4 at $t = 0.5$ h.

faults d_2 or d_4. At this time, the system operator can utilize the partial isolation to examine the plant and determine the exact source of the failure. The manipulated input for this scenario can be seen in Figure 16.

4. Conclusions

This work addressed the problem of fault detection and isolation and fault-tolerant control when several process measurements are not available synchronously. First, an FDI scheme that employs model-based techniques was proposed that allowed for the isolation of faults. This scheme employed model-based FDI filters in addition to observers that estimate the fault-free evolution of asynchronously measured states during times when they are unmeasured. Specifically, the proposed FDI scheme provides detection and isolation for a type I fault where the fault enters into the differential equation of only synchronously measured states, and grouping of type II faults where the fault enters into the differential equation of any asynchronously measured state. The detection occurs shortly after a fault takes place, and the isolation, limited by the arrival of asynchronous measurements, occurs once all of the asynchronous measurements become available. Once the FDI methodology provided the system supervisor with a fault diagnosis, the supervisor took appropriate action to seamlessly reconfigure the system to an alternative control configuration that enforces the desired operation. We presented applications of the proposed asynchronous FDI and FTC framework to a polyethylene reactor simulation.

Literature Cited

(1) Nimmo, I. Adequately Address Abnormal Operations. *Chem. Eng. Prog.* **1995**, *91*, 36–45.

(2) Whiteley, J. R.; Davis, J. F. Qualitative Interpretation of Sensor Patterns. *IEEE Expert* **1992**, *8*, 54–63.

(3) Bakshi, B. R. Multiscale PCA with Application to Multivariate Statistical Process Monitoring. *AIChE J.* **1998**, *44*, 1596–1610.

(4) Davis, J. F.; Piovoso, M. L.; Kosanovich, K.; Bakshi, B. Process Data Analysis and Interpretation. *Adv. Chem. Eng.* **1999**, *25*, 1–103.

(5) Polycarpou, M. M.; Trunov, A. B. Learning approach to nonlinear fault diagnosis: Detectability analysis. *IEEE Trans. Autom. Control* **2000**, *45*, 806–812.

(6) Polycarpou, M. M. Fault accommodation of a class of multivariable nonlinear dynamical systems using a learning approach. *IEEE Trans. Autom. Control* **2001**, *46*, 736–742.

(7) Tatara, E.; Cinar, A. An intelligent system for multivariate statistical process monitoring and diagnosis. *ISA Trans.* **2002**, *41*, 255–270.

(8) Nounou, M. N.; Bakshi, B. R.; Goel, P. K.; Shen, X. Bayesian Principal Component Analysis. *J. Chemom.* **2002**, *16*, 576–595.

(9) Aradhye, H. B.; Davis, J. F.; Bakshi, B. R. ART-2 and Multiscale ART-2 for On-Line Process Fault Detection- Validation via Industrial Case Studies and Monte Carlo Simulation. *Annu. Rev. Control* **2002**, *26*, 113–127.

(10) Venkatasubramanian, V.; Rengaswamy, R.; Yin, K.; Kavuri, S. N. Review of Process Fault Diagnosis- Parts I, II, III. *Comput. Chem. Eng.* **2003**, *27*, 293–346.

(11) Aradhye, H. B.; Bakshi, B. R.; Davis, J. F.; Ahalt, S. C. Clustering in Wavelet Domain: A Multiresolution ART Network for Anomaly Detection. *AIChE J.* **2004**, *50*, 2455–2466.

(12) Zhang, X. D.; Parisini, T.; Polycarpou, M. M. Adaptive fault-tolerant control of nonlinear uncertain systems: An information-based diagnostic approach. *IEEE Trans. Autom. Control* **2004**, *49*, 1259–1274.

(13) Ohran, B.; Muñoz de la Peña, D.; Christofides, P. D.; Davis, J. F. Enhancing data-based fault isolation through nonlinear control. *AIChE J.* **2008**, *53*, 2734–2741.

(14) Massoumnia, M.; Verghese, G. C.; Wilsky, A. S. Failure detection and identification. *IEEE Trans. Autom. Control* **1989**, *34*, 316–321.

(15) Frank, P. M. Fault Diagnosis in Dynamic Systems Using Analytical and Knowledge-based Redundancy-- A Survey and Some New Results. *Automatica* **1990**, *26*, 459–474.

(16) Garcia, E. A.; Frank, P. M. Deterministic Nonlinear Observer-Based Approaches to Fault Diagnosis: A Survey. *Control Eng. Pract.* **1997**, *5*, 663–670.

(17) Frank, P. M.; Ding, X. Survey of Robust Residual Generation and Evaluation Methods in Observer-based Fault Detection Systems. *J. Proc. Control* **1997**, *7*, 403–424.

(18) Zad, S. H.; Massoumnia, M. Generic solvability of the failure detection and identification problem. *Automatica* **1999**, *35*, 887–893.

(19) Niemann, H.; Saberi, A.; Stoorvogel, A. A.; Sannuti, P. Exact, almost and delayed fault detection- an observer based approach. *Int. J. Robust Nonlinear Control* **1999**, *9*, 215–238.

(20) Saberi, A.; Stoorvogel, A. A.; Sannuti, P.; Niemann, H. Fundamental problems in fault detection and identification. *Int. J. Robust Nonlinear Control* **2000**, *10*, 1209–1236.

(21) Mhaskar, P.; McFall, C.; Gani, A.; Christofides, P.; Davis, J. Isolation and Handling of Actuator Faults in Nonlinear Systems. *Automatica* **2008**, *44*, 53–62.

(22) Mhaskar, P.; Gani, A.; El-Farra, N. H.; Christofides, P. D.; Davis, J. F. Integrated Fault-Detection and Fault-Tolerant Control of Process Systems. *AIChE J.* **2006**, *52*, 2129–2148.

(23) DePersis, C.; Isidori, A. A Geometric Approach to Nonlinear Fault Detection and Isolation. *IEEE Trans. Autom. Control* **2001**, *46*, 853–865.

(24) Armaou, A.; Demetriou, M. Robust Detection and Accomodation of Incipient Component and Actuator Faults in Nonlinear Distributed Processes. *AIChE J.* **2008**, *54*, 2651–2662.

(25) Mhaskar, P.; Gani, A.; McFall, C.; Christofides, P. D.; Davis, J. F. Fault-Tolerant Control of Nonlinear Process Systems Subject to Sensor Faults. *AIChE J.* **2007**, *53*, 654–668.

(26) El-Farra, N. H.; Gani, A.; Christofides, P. D. Fault-Tolerant Control of Process Systems using communication Networks. *AIChE J.* **2005**, *51*, 1665–1682.

(27) Muñoz de la Peña, D.; Christofides, P. D. Lyapunov-Based Model Predictive Control of Nonlinear Systems Subject to Data Losses. *IEEE Trans. Autom. Control* **2008**, *53*, 2076–2089.

(28) Muñoz de la Peña, D.; Christofides, P. D. Output Feedback Control of Nonlinear Systems Subject to Sensor Data Losses. *Syst. Control Lett.* **2008**, *57*, 631–642.

(29) Yang, G. H.; Zhang, S. Y.; Lam, J.; Wang, J. Reliable Control Using Redundant Controllers. *IEEE Trans. Autom. Control* **1998**, *43*, 1588–1593.

(30) Siljak, D. D. Reliable control using multiple control systems. *Int. J. Control* **1980**, *31*, 302–339.

(31) Yang, G. H.; Wang, J. L.; Soh, Y. C. Reliable H ∞ control design for linear systems. *Automatica* **2001**, *37*, 717–725.

(32) Mhaskar, P.; Gani, A.; Christofides, P. D. Fault-Tolerant Control of Nonlinear Processes: Performance-Based Reconfiguration and Robustness. *Int. J. Robust Nonlinear Control* **2006**, *16*, 91–111.

(33) McAuley, K. B.; Macdonald, D. A.; McLellan, P. J. Effects of Operating Conditions on Stability of Gas-Phase Polyethylene Reactors. *AIChE J.* **1995**, *41*, 868–879.

(34) Gani, A.; Mhaskar, P.; Christofides, P. D. Fault-tolerant control of a polyethylene reactor. *J. Process Control* **2007**, *17*, 439–451.

(35) Kokotovic, P.; Arcak, M. Constructive nonlinear control: a historical perspective. *Automatica* **2001**, 637–662.

(36) Christofides, P. D.; El-Farra, N. H. *Control of Nonlinear and Hybrid Process Systems: Designs for Uncertainty, Constraints and Time-Delays*; Springer-Verlag: Berlin, Germany, 2005.

(37) Sontag, E. A 'universal' construction of Arstein's theorem on nonlinear stabilization. *Syst. Control Lett.* **1989**, 117–123.

(38) Walsh, G.; Beldiman, O.; Bushnell, L. Asymptotic Behavior of nonlinear networked control systems. *IEEE Trans. Autom. Control* **2001**, *46*, 1093–1097.

(39) Walsh, G.; Ye, H.; Bushnell, L. Stability analysis of networked control systems. *IEEE Trans. Control Syst. Technol.* **2002**, *10*, 438–446.

(40) Nesic, D.; Teel, A. R. Input-to-state stability of networked control systems. *Automatica* **2004**, *40*, 2121–2128.

(41) Nesic, D.; Teel, A. R. Input-Output Stability Properties of Networked Control Systems. *IEEE Trans. Autom. Control* **2004**, *49*, 1650–1667.

(42) Dadebo, S. A.; Bell, M. L.; McLellan, P. J.; McAuley, K. B. Temperature Control of Industrial Gas Phase Polyethylene Reactors. *J. Process Control* **1997**, *7*, 83–95.

(43) El-Farra, N. H.; Christofides, P. D. Integrating Robustness, Optimality, and Constraints in Control of Nonlinear Processes. *Chem. Eng. Sci.* **2001**, *56*, 1841–1868.

Received for review July 9, 2008
Revised manuscript received September 24, 2008
Accepted October 6, 2008

IE801056Y